Highly efficient silicon mode converter and polarization rotator using a silicon-based hybrid plasmonic waveguide

BASMA E. ABU-ELMAATY[1],* (iD) AND HOSSAM M. H. SHALABY[2] (iD)

[1]*Electrical Engineering Department, Faculty of Engineering, Tanta University, Tanta, Egypt*
[2]*Electrical Engineering Department, Faculty of Engineering, Alexandria University, Alexandria 21544, Egypt*
*eng.basma_eldsouky@f-eng.tanta.edu.eg

We propose and numerically analyze a broadband, ultracompact hybrid plasmonic mode converter/polarization rotator. The proposed device converts the fundamental transverse magnetic mode (TM_0) to the first-order transverse electric mode (TE_1). The mode converter is designed using a tapered hybrid plasmonic waveguide in which metal parts are directly surrounding both the input Si waveguide and the tapered output waveguide without a thin low-index layer. After optimizing the proposed structure, a TM_0-to-TE_1 mode converter with a modal conversion efficiency of 98.2% is achieved. A broad operating bandwidth of 100 nm is achieved with a compact footprint of only 0.8 µm × 12.5 µm for the whole device. At a wavelength of 1550 nm, the insertion loss ranges from 0.91 dB to 1.19 dB using different metal materials, and the extinction ratio of the TE_1 and TM_0 modes is higher than 21 dB in the output Si waveguide. © 2023 Optica Publishing Group

1. INTRODUCTION

On-chip mode converters and polarization rotators play a significant role in multiplexing techniques, with the rapid growth of silicon photonics integrated circuits (SPIC) [1,2]. Mode-division multiplexing (MDM) [3] and simultaneous mode and polarization-division-multiplexing (PDM-MDM) techniques are powerful and promising techniques to increase data capacity in on-chip optical communications systems [4,5]. Indeed, expanding the number of modes that can be used in MDM systems can improve the on-chip transmission capacity of photonic systems [6]. In addition, keeping both polarized TE and TM modes, rather than focusing on using one of them, doubles the transmission capacity by allowing two different data streams to be transmitted through a single mode. This can be accomplished by merging the PDM with another type of multiplexing technique [7]. Compared to using each approach individually, these hybrid multiplexing methods offer higher data rates.

These methods typically necessitate mode conversion from lower fundamental modes to higher-order modes before multiplexing different data channels on a single multimode channel [8]. Mode converters play a crucial role in facilitating the conversion between various optical modes, allowing efficient multiplexing and demultiplexing of signals transmitted through individual modes, therefore enhancing the performance, compatibility, and versatility of optical systems across a wide range of applications [9]. MDM has the potential to

significantly enhance data transmission rates and bandwidth in optical networks. Therefore, mode converters, especially polarization rotators, play an important role in PDM-MDM systems [10]. However, few studies have been done on polarization mode conversion from the fundamental TE/TM mode to a higher-order TM/TE mode in a single silicon waveguide platform. This kind of conversion is not only useful for MDM systems but is also crucial and very important for other photonic devices, such as polarization splitters/rotators and mode filters [11,12]. Different schemes have been reported using various conversion techniques and structures [8,13,14]. Among these works, a polarization rotator has been proposed on the silicon-on-insulator (SoI) platform for conversion from the TM_0 mode to the TE_0 mode using both straight and bent multimode waveguides. This structure has a low insertion loss of 0.86 dB, and the total device size is 19.5 µm [15].

Structures for tapered plasmonic mode converters have also been proposed. A hybrid plasmonic TE_0 to TM_1 polarization rotator has been reported with an insertion loss of 2.34 dB and a mode conversion purity of 94.6% [16]. This structure was formed by a multimode hybrid plasmonic slot waveguide (HPSW) with two straight gold layers symmetrically placed beside the silicon sidewalls with a total footprint of 2.33×7 µm². A tapered silicon rib waveguide was used for the conversion of the TM_0 mode to higher-order TE modes in [17], and another taper mode converter structure with angled sidewalls was reported in [18,19]. The tapered waveguide-based

mode converter is the most common method used for high conversion efficiency with low losses. However, taper-based structures have a major drawback: a relatively large device size.

In this paper, we propose a hybrid plasmonic taper waveguide (HPTW) structure to form a polarization rotation from the TM_0 mode to the TE_1 mode. It relies on the mode hybridization principle in a taper hybrid plasmonic waveguide without a thin low-index layer. We introduce what we believe, to the best of our knowledge, is a new device structure by introducing four silver metal parts placed symmetrically around the straight input and the taper output waveguides. The proposed mode converter's overall footprint is very compact, measuring only 0.8×12.5 μm^2. After analyzing the surrounded metal parts of the silicon waveguides in detail, we developed a TM_0-to-TE_1 plasmonic mode-order converter with a conversion efficiency, insertion loss, and crosstalk of 98.2%, 1.19 dB, and 21.1 dB, respectively, at a 1.55 μm wavelength.

2. DEVICE STRUCTURE AND PRINCIPLE

Figure 1 shows the structure layout of the proposed ultracompact TM_0-to-TE_1 mode converter. The entire device is built on a silicon-on-insulator (SoI) platform with an upper cladding of SiO_2, and a silicon thickness of H_{Si}. At a 1550 nm wavelength, the refractive indices of SiO_2 and Si are 1.44 and 3.47, respectively. The mode conversion section, which is the central portion of the device, is made up of a multimode HPTW with two cascaded waveguides; the input straight waveguide has a width W_1, and the taper output waveguide has a width W_2. To achieve an effective conversion from the input TM_0 to the output TE_1 mode in an ultracompact size, we developed a hybrid plasmonic structure that may significantly influence the optical mode properties during the propagation of light. Accordingly, both the input and output waveguides are surrounded by two cascaded metal strips of lengths L_1 and L_2 and a uniform thickness H_m, placed symmetrically alongside the silicon sidewalls. The suggested device's fundamental component is its metal structure, whose size and shape must be carefully considered. In our analysis, we chose a refractive index of the silver (Ag) metal to be $0.474 + 13.52i$ at a wavelength of 1.55 μm [20].

The working principle of the suggested device is based on the TM_0-to-TE_1 polarization rotation (PR), which is supported by the surrounding optimized metal parts. The input TM_0 mode can travel steadily along the silicon nanowire after being launched into it before it reaches the region of mode conversion.

If no perturbation is introduced to the symmetry in a single optical waveguide in one direction, the modes will retain their

symmetries in this direction along the waveguide; therefore, the modes cannot be converted.

In addition, from our initial analysss, we found that for the PR structure, its cross shape must be asymmetrical in the height direction. For the conversion from the TM_0 mode to the TE_1 mode, we must introduce a perturbation in the traditional nanowire as well as break the symmetry in the height direction. Therefore, the metal taper has been used to provide a perturbation in the height directions to provide a mode hybridization region for the occurrence of the mode conversion between the TM_0 mode and the high-order TE_1 mode with a very compact structure and high fabrication tolerance. We further improve the device parameters based on this design structure to obtain the optimum dimensions to get an effective TM_0-to-TE_1 mode-order converter in a relatively small length.

3. RESULTS AND DISCUSSION

Before we conducted the device design and analysis, we determined the sizes of both input and output silicon multimode waveguides. Figure 2 shows the calculated effective indices for all guided modes supported in an SoI strip waveguide with different widths ranging from 0.4 μm to 1.6 μm, with a silicon thickness H_{Si} of 300 nm, using the effective index method (EIM) [21,22]. Both the upper- and lower-cladding are chosen to be SiO_2; thus, the SoI nanowire becomes a regular strip waveguide, which is symmetrical in the vertical direction.

Note that in the region marked by the dotted circle, the two curves for TM_0, and TE_1 just cross each other and there is no gap between them. When using surrounding metal strips, an asymmetrical waveguide structure is introduced in the vertical direction, and the two curves for TM_0 and TE_1 become close to each other [16,23]. These two closely spaced curves continue to anti-crossing, and there is a slight gap between them, which introduces a mode hybridization region around the width W of 0.85 μm [15]. Compared to the dielectric silicon strip waveguide, the introduction of a metal plasmonic structure can significantly affect and alter the waveguide modes and transmission characteristics, resulting in a smaller device footprint with improved performance. The mode conversion between the two hybridized modes would happen when the light propagates along a short plasmonic taper structure whose end widths are chosen as $W_1 = 0.8$ μm and $W_2 = 1.4$ μm when launching the TM_0 mode. Mode hybridization in other SoI waveguides with vertical asymmetry has also been observed theoretically and experimentally in previous literature [15,18]. The widths of the input waveguide and output waveguide are chosen to be
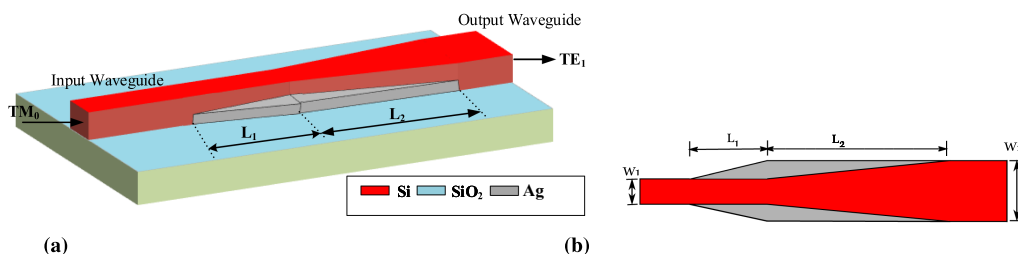

Fig. 1. Schematic structure of proposed TM_0-to-TE_1 HPMC: (a) side schematic view and (b) top view of the central area (conversion section).
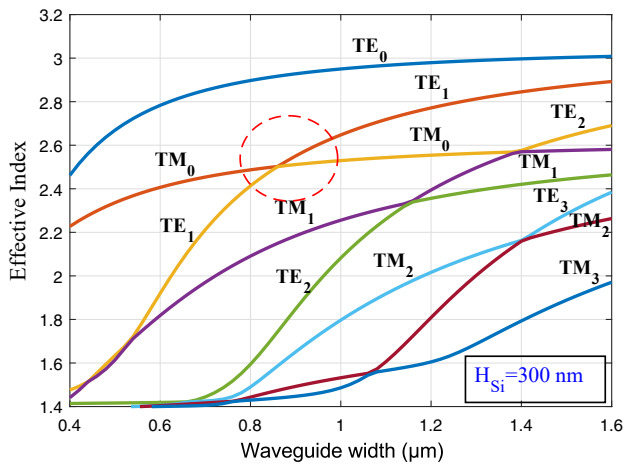
Fig. 2. Effective indices for the eigenmodes of SoI nanowires with Si layer height of $H_{Si} = 300$ nm and SiO$_2$ cladding.

$W_1 = 0.8$ μm and $W_2 = 1.4$ μm, respectively, to ensure the desired TM$_0$-TE$_1$ hybridization at the output port.

The polarization rotator, as described in [17,24], also can be achieved using slab structures. These structures exhibit an asymmetrical cross shape in terms of height and introduce a mode hybridization region that facilitates the conversion between the TM and TE modes. The use of these structures comes with the disadvantage of requiring a very long taper (with a length of $L_c \geq 200$ μm) for adiabatic conversion. A recently developed approach to create an asymmetric perturbation is through the use of a surface plasmon polarizer structure. A tapered hybrid plasmonic waveguide has recently been employed to achieve a highly compact size with ($L_c \leq 15$ μm) [10,23].

Using the details provided, this Letter introduces a hybrid plasmonic taper waveguide (HPTW) structure designed to convert the TM$_0$ mode to the TE$_1$ mode. The proposed converter takes advantage of the mode-interference principle, enabling a significant reduction in size. Specifically, the footprint of the proposed polarizer described here can be minimized to just 12.5 μm.

To obtain the optimal device parameters, the proposed structure was simulated using Lumerical software. This software is employed to conduct simulations and analyze the device performance. The proposed structure was simulated with SiO$_2$ cladding and buried oxide of 2 μm. We swept the lengths of the two cascaded metal tapers L_1 and L_2, and their uniform thickness H_m for an acceptable conversion loss and high conversion efficiency from the TM$_0$ mode to the high-order TE$_1$ mode with a minimized device size. We found two optimum parameter groups; both achieve mode conversion with acceptable conversion efficiencies. The first optimum parameters are $L_1 = 3$ μm, $L_2 = 6.5$ μm, and $H_m = 75$ nm; the second optimum values are $L_1 = 2$ μm, $L_2 = 10.5$ μm, and $H_m = 75$ nm.

To gain a deeper insight into the mode conversion process, the distribution of the electric field for forward propagation in the HPTW is depicted in Fig. 3. As the length of the surrounding metal tapers increases, the input TM$_0$ mode is observed to gradually convert into the TE$_1$ mode. By analyzing the distribution of the electric field at the corresponding locations displayed in Fig. 3(a), the input TM$_0$ mode in the silicon waveguide is first coupled into the plasmonic TM$_0$ mode in the hybrid plasmonic waveguide [see Fig. 3(c)], after which it begins to become a hybrid mode due to the interaction between the metal parts and the silicon waveguide interface [see Fig. 3(d)]. Then, it converts into a hybrid mode that exhibits characteristics similar to the
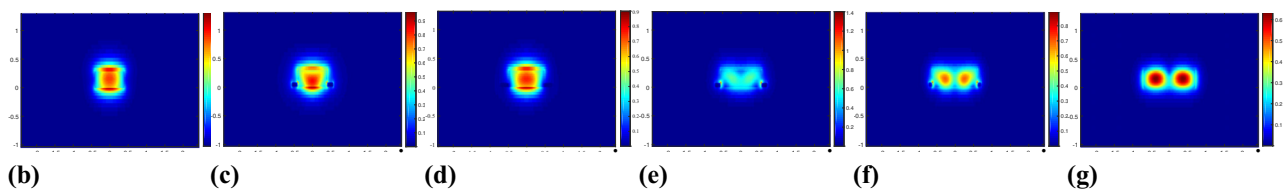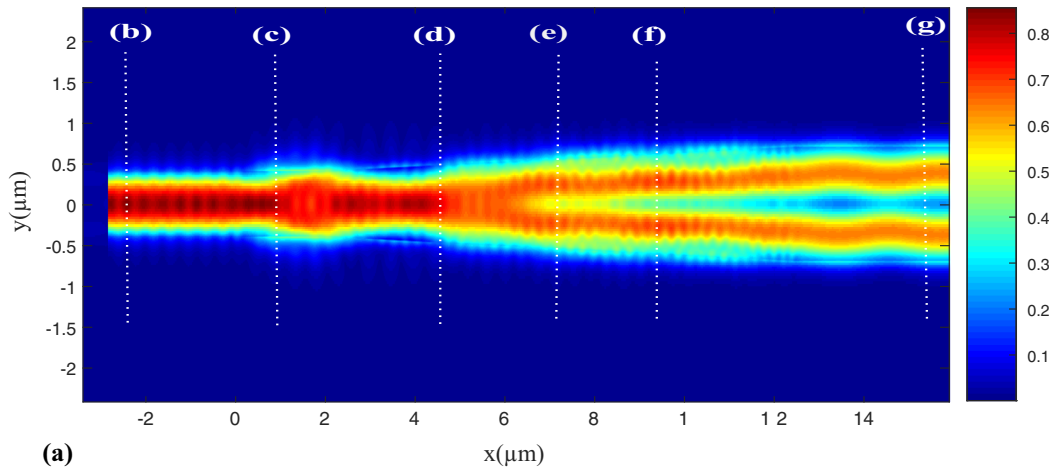

Fig. 3. (a) Distribution of the electric field in the hybrid plasmonic waveguide with the TM$_0$ mode input in the forward direction. (b)–(g) Cross-sectional electric field profile at the respective locations (white dot lines).

TE_1 mode at the end of the metal [see Fig. 3(f)]. Eventually, it couples out as the TE_1 mode in the silicon waveguide [see Fig. 3(g)]. This means that the electromagnetic field undergoes various transformations and interactions with the hybrid plasmonic taper waveguide, then eventually emerges from the structure and exhibits characteristics typical of the TE_1 mode in the dielectric waveguide.

A. Performance Analysis

The performance of the suggested first-order PR mode converter is analyzed and simulated using 3D-FDTD Solutions. The obtained parameters in the previous subsection are used in our simulation. The device's performance is determined in terms of its modal conversion efficiency (CE), insertion loss (IL), and crosstalk (CT), defined as

$$\mathrm{IL} = 10\log_{10}\frac{P_{\mathrm{TE}_1}}{P_{\mathrm{IN}}},$$

$$\mathrm{CT} = 10\log_{10}\frac{P_{\mathrm{OIM}}}{P_{\mathrm{IN}}},$$

$$\mathrm{CE} = \frac{P_{\mathrm{TE}_1}}{P_{\mathrm{OUT}}} \times 100\%, \qquad (1)$$

respectively, where P_{TE_1}, P_{IN}, P_{OUT}, and P_{OIM} are the output power of the desired TE_1 mode, the total power at the input port, the total received power at the output port, and the received power of the other undesirable mode at the output port, respectively.

The use of Lumerical software has been documented to conduct 3D-FDTD simulations with a mesh accuracy of 3 and PML boundary conditions. The results obtained while employing Ag (silver) material are presented in Fig. 4(a) when simulating the proposed device using the first optimum parameters of $L_1 = 3$ μm, $L_2 = 6.5$ μm, and $H_m = 75$ μm. The figure clearly shows that the conversion into TE_1 mode occurred at 1550 nm with a high IL of -1.39 dB and an acceptable CT of -9.8 dB and -22.69 dB to both fundamental TM_0 and second-order TM_2 modes.

The reported mode converter's 3D-FDTD field propagation is depicted in Fig. 5 when exciting the device by a TM_0 mode at

the input waveguide. After going through the metal strips, there is a distinct conversion to the TE_1 mode.

These design parameters achieve a good conversion efficiency of about 87% to the first-order TE_1 mode with a compact footprint of the whole mode converter of only 0.8 μm × 9.5 μm. However, the device structure in this case has a lower extinction ratio (ER) of about 8.4 dB, where the extinction ratio is defined as

$$\mathrm{ER} = \mathrm{IL}_{\mathrm{TE}_1} - \mathrm{CT}_{\mathrm{TM}_0}. \qquad (2)$$

B. Extinction Ratio Improvement

To improve the extinction ratio between the TE_1 and TM_0 modes of our proposed PR, we slightly increased the footprint of the proposed structure to be 0.8 μm × 12.5 μm. We did this by using the second optimum parameters of $L_1 = 2$ μm, $L_2 = 10.5$ μm, and $H_m = 75$ nm. These parameters also realized the mode conversion into the first-order TE_1 mode, as shown in Fig. 4(b). The results indicate that the mode conversion was achieved over a wide bandwidth with an IL of -1.19 dB, and CTs of -21.11 dB and -30.32 dB to both the fundamental TM_0 and second-order TM_2 modes, respectively, at 1550 nm.

These design parameters achieve a conversion efficiency of 98.2% to the first-order TE_1 mode with a compact footprint of only 0.8 μm × 12.5 μm of the whole mode converter. The device structure in this case has a higher extinction ratio (ER) of 20 dB.

C. Fabrication Tolerance Analysis

Finally, the fabrication tolerance of the proposed hybrid plasmonic mode converter is examined in this subsection. Since the plasmonic-based devices are very sensitive to dimension deviations, we assume that the central positions of silicon waveguides are accurate. As the width of the metal strips depends on the widths of the input and output waveguides W_1 and W_2, respectively, we just consider that the widths of the silicon waveguides are only changed by ΔW_1 and ΔW_2 to evaluate the fabrication tolerance. Considering the decline in device performance induced by fabrication defects in practice, we investigated the
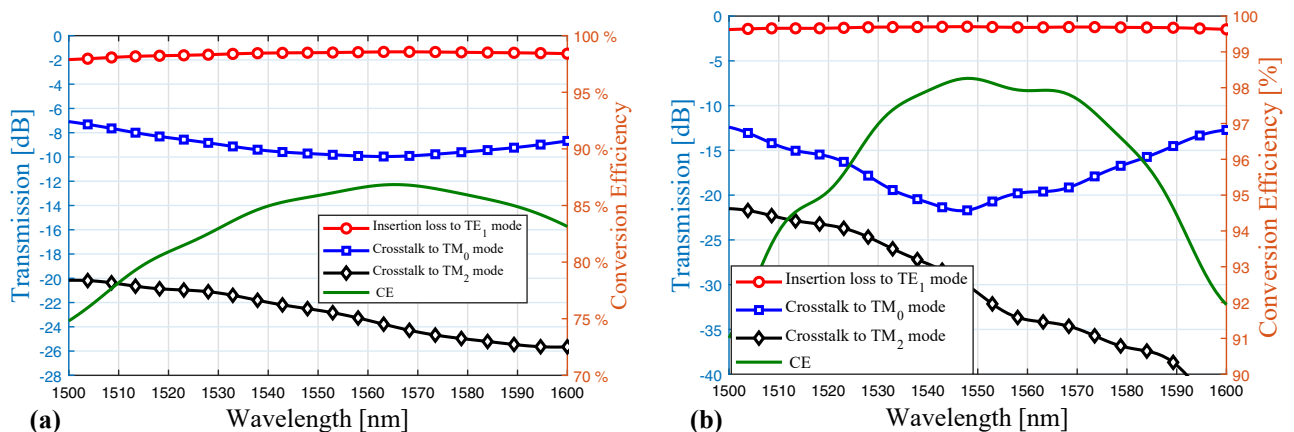

Fig. 4. Wavelength dependency of the proposed mode-order converter's modal IL, CT, and CE at device parameters of (a) $L_1 = 3$ μm, $L_2 = 6.5$ μm, and $H_m = 75$ nm and (b) $L_1 = 2$ μm, $L_2 = 10.5$ μm, and $H_m = 75$ nm.
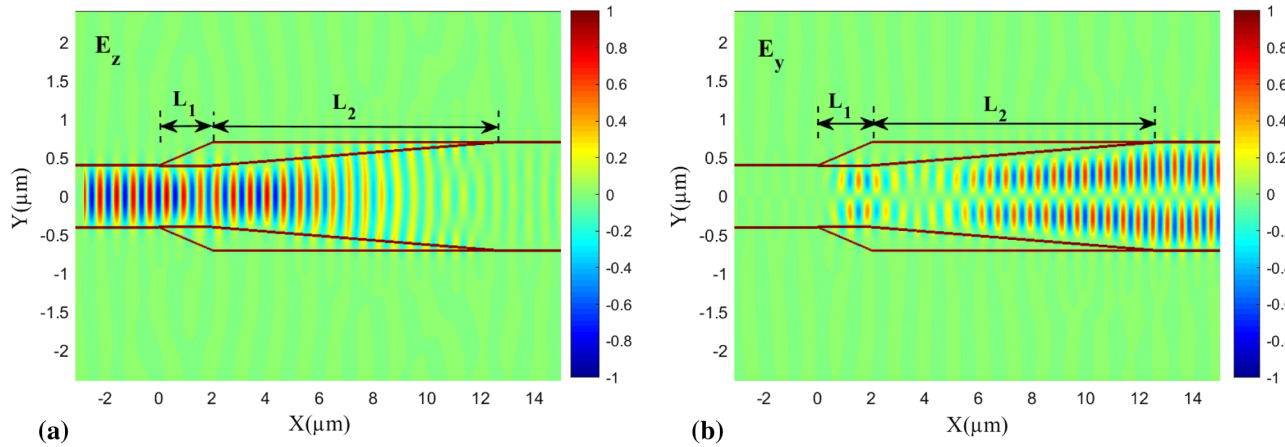
Fig. 5. Electric field propagation of input TM_0 mode (along x propagation direction) of designed TM_0-to-TE_1 mode-order converter with surrounding metal tapers. Both major and minor electric field components, (a) E_z and (b) E_y, are plotted.
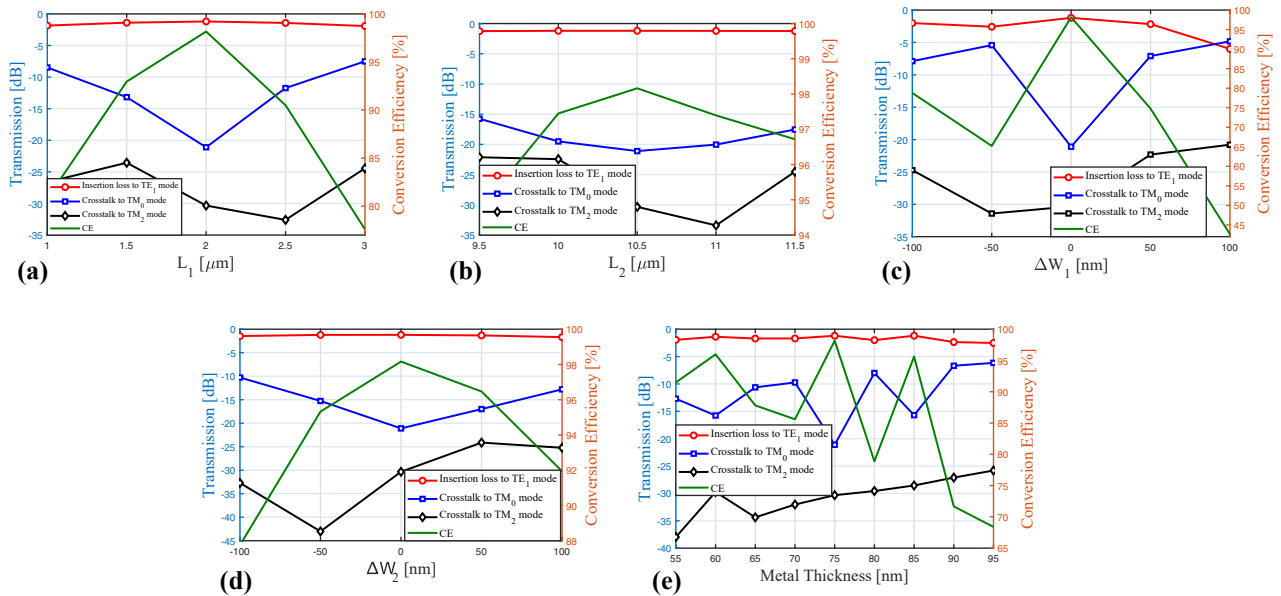

Fig. 6. Manufacturing tolerance analysis of the reported mode-order converter by taking into account the following parameters: (a) length L_1 of the first metal part, (b) length L_2 of the second metal part, (c) width deviation ΔW_1 of the input waveguide, (d) width deviation ΔW_2 of the output waveguide, and (e) metal thickness.

fabrication tolerance of several key structural parameters, such as L_1, L_2, H_m, ΔW_1, and ΔW_2, as illustrated in Fig. 6. In this figure, the modal CE, IL, and CT of the proposed device are evaluated.

The analysis results illustrate that the device performance is relatively insensitive to slight variations in the thickness and lengths of the metal parts H_m, L_1, and L_2. The lengths L_1 and L_2 can be shifted within the ranges of [1 µm to 3 µm] and [9.5 µm to 11.5 µm], respectively, while the metal thickness has an acceptable conversion efficiency of [80% to 98.2%] within the range of [55 nm to 85 nm]. In the fabrication process, the metal parts are deposited on the substrate using electron-beam evaporation, and thickness can be placed at any oxide depth for electrical and optical circuits or custom heaters [25]. The metal thickness in the proposed structure can be controlled to an accuracy of ±5% of the overall thickness [26]. In addition, the

width deviation of the output waveguide ΔW_2 also has a little impact on the device performance within the range [1.3 µm to 1.5 µm], while the CE ranged from [88% to 98.2%].

However, the analysis results depict that the width variation of the input waveguide ΔW_1 has a remarkable impact on the ER, as the ER can be shifted from [20 dB to 2.9 dB] while the CE changes from 65% to 98.2%. The variation of the waveguide width or height affects the device performance and produces a 1 nm or 2 nm spectral shift, respectively. This extreme level of dimensional control in the input waveguide width can be achieved and controlled using electron beam lithography technology with high-resolution features and small spacings of 60 nm [25]. Due to the rapid progress in silicon photonics fabrication technologies, the minimum feature size of the fabricated structures will be less than 30 nm in the next decade [26].

Table 1.   Comparison of Various Mode Converters

Reference	Function	Length (μm)	IL (dB)	CE (%)
Tapered silicon ridge waveguide [19]	TM_0-to-TE_1	≥ 250		≈ 100
Tapered waveguide with angled sidewalls [18]	TM_0-to-TE_1	≥ 200		≈ 100
Multimode waveguide PR [15]	TM_0-to-TE_0	19.5	0.82	ER = 25.8 dB
InGaAs-InP based mode converter [29]	TM_0-to-TE_0	2.5 (mm)		90
Tapered plasmonic waveguide [30]	TE_0-to-TM_1	11	4.2	ER $\geq$ 20(dB)
Metal plasmonic waveguide [10]	TE_0-to-TM_1	3.5	2.7	94.2%
Hybrid plasmonic slot waveguide [16]	TE_0-to-TM_1	7	$\leq$2.34	94.6%
Our work	TM_0-to-TE_1	12.5	0.91	98.2
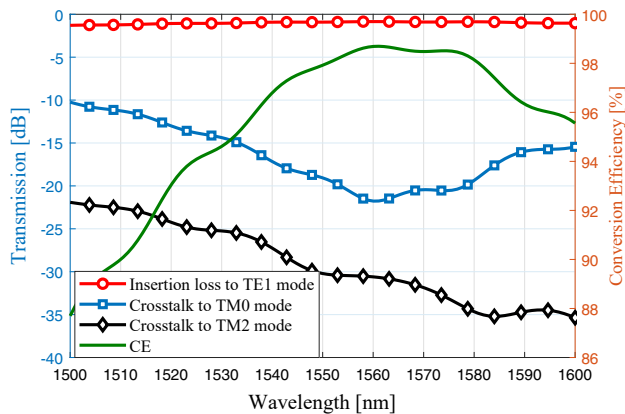
Fig. 7.   Wavelength dependency of the proposed mode-order converter's modal IL, CT, and CE using Au (gold) material at device parameters of $L_1 = 2$ μm, $L_2 = 10.5$ μm, and $H_m = 75$ nm.

D. Device Performance Using Gold Material

In this section, we evaluate the proposed structure using another metal material of gold (Au) with a refractive index of $0.23823 + 11.263i$ at a wavelength of 1.55 μm [27].

The 3D-FDTD simulation results when using Au material are shown in Fig. 7 when simulating the proposed device using the optimum parameters of $L_1 = 2$ μm, $L_2 = 10.5$ μm, and $H_m = 75$ nm. The figure clearly indicates that the conversion into the TE_1 mode is completed at 1550 nm with a very high IL of -0.91 dB and an acceptable CT of -19 dB and -30.2 dB to the both fundamental TM_0 and second-order TM_2 modes. These design parameters achieve a conversion efficiency of 98% to the first-order TE_1 mode using Au material. The device structure in this case has a higher extinction ratio (ER) of 18.1 dB.

The previous results demonstrate that the performance of the reported device using silver and gold materials is extremely close. For both Au and Ag metal materials, the IL and CE range from 0.91 dB to 1.19 dB and from 98% to 98.2%, respectively. Since the thickness thresholds of Ag and Au are, respectively, 12–23 nm and 1.5–7 nm [28], both materials are appropriate to form metal layers with a thickness of 75 nm for fabrication of the proposed device. A final material selection necessitates a trade-off between the cost and manufacturing ease.

At the operational wavelength, the refractive indices of Ag and Au differ from one another. As a result, each material has different optical properties and propagation losses, which causes

this variation in the device performance parameters (IL, CT, and CE).

Table 1 contrasts our suggested device with a number of other reported mode converters with several different device structures. It shows that the suggested mode converter has a shorter length than the earlier experimental results and a higher conversion efficiency.

4. CONCLUSION

In this research, we developed and presented a polarization rotator to achieve mode conversion between the TM_0 and TE_1 modes using a new tapered hybrid plasmonic waveguide structure. The mode converter is formed by using very short tapered strips of silver material surrounding both the straight input and the tapered output waveguides. The device length is only 12.5 μm, and the mode conversion has been achieved to TE_1 with an IL ranges from 0.91 dB to 1.19 dB for both Au and Ag metal materials, respectively, over a broad operating spectrum of 100 nm. The reported mode-order converter's obtained modal CE and CT are 98.2%, -20.11 dB, and -30.32 dB to both the TM_0 and TM_2 modes, respectively, at 1550 nm. Moreover, the structure fabrication tolerance has been demonstrated. Furthermore, the suggested device architecture offers a good device performance, an ultracompact size, and scalability, making it a strong candidate to boost transmission capacity in on-chip compact PDM-MDM systems by incorporating additional polarization mode channels.

REFERENCES

1. Y. Xiong, R. B. Priti, and O. Liboiron-Ladouceur, "High-speed two-mode switch for mode-division multiplexing optical networks," Optica **4**, 1098–1102 (2017).
2. D. González-Andrade, J. G. Wangüemert-Pérez, A. V. Velasco, A. Ortega-Monux, A. Herrero-Bermello, I. Molina-Fernandez, R. Halir, and P. Cheben, "Ultra-broadband mode converter and multiplexer based on sub-wavelength structures," IEEE Photon. J. **10**, 2201010 (2018).
3. H. M. Shalaby, "Bidirectional mode-division multiplexers with antireflection gratings," Appl. Opt. **57**, 476–484 (2018).
4. K. Chen, S. Wang, S. Chen, S. Wang, C. Zhang, D. Dai, and L. Liu, "Experimental demonstration of simultaneous mode and polarization-division multiplexing based on silicon densely packed waveguide array," Opt. Lett. **40**, 4655–4658 (2015).

5. X. Han, Y. Jiang, A. Frigg, H. Xiao, P. Zhang, T. G. Nguyen, A. Boes, J. Yang, G. Ren, Y. Su, A. Mitchell, and Y. Tian, "Mode and polarization-division multiplexing based on silicon nitride loaded lithium niobate on insulator platform," Laser Photon. Rev. **16**, 2100529 (2022).

6. J. Wang, S. He, and D. Dai, "On-chip silicon 8-channel hybrid (de) multiplexer enabling simultaneous mode-and polarization-division-multiplexing," Laser Photon. Rev. **8**, L18–L22 (2014).

7. S. N. Khonina, N. L. Kazanskiy, M. A. Butt, and S. V. Karpeev, "Optical multiplexing techniques and their marriage for on-chip and optical fiber communication: a review," Opto-Electron. Adv. **5**, 210127 (2022).

8. B. E. Abu-Elmaaty, M. S. Sayed, R. K. Pokharel, and H. M. Shalaby, "General silicon-on-insulator higher-order mode converter based on substrip dielectric waveguides," Appl. Opt. **58**, 1763–1771 (2019).

9. H. Wang, Y. Zhang, Y. He, Q. Zhu, L. Sun, and Y. Su, "Compact silicon waveguide mode converter employing dielectric metasurface structure," Adv. Opt. Mater. **7**, 1801191 (2019).

10. Y. Xu, L. Liu, X. Hu, Y. Dong, B. Zhang, and Y. Ni, "Metal plasmonic assisted silicon-based Te_0-to-Tm_1 mode-order converter with 3.5 μm length," Opt. Laser Technol. **142**, 107251 (2021).

11. D. Liu, H. Xu, Y. Tan, Y. Shi, and D. Dai, "Silicon photonic filters," Microw. Opt. Technol. Lett. **63**, 2252–2268 (2021).

12. W. Zhou, Y. Tong, X. Sun, and H. K. Tsang, "Ultra-broadband hyperuniform disordered silicon photonic polarizers," IEEE J. Sel. Top. Quantum Electron. **26**, 8201109 (2019).

13. R. Xiao, Y. Shi, J. Li, P. Dai, Y. Zhao, L. Li, J. Lu, and X. Chen, "On-chip mode converter based on two cascaded Bragg gratings," Opt. Express **27**, 1941–1957 (2019).

14. L. Hao, R. Xiao, Y. Shi, P. Dai, Y. Zhao, S. Liu, J. Lu, and X. Chen, "Efficient TE-polarized mode-order converter based on high-index-contrast polygonal slot in a silicon-on-insulator waveguide," IEEE Photon. J. **11**, 6601210 (2019).

15. H. Xu and Y. Shi, "Ultra-compact and highly efficient polarization rotator utilizing multi-mode waveguides," Opt. Lett. **42**, 771–774 (2017).

16. R. Chen, B. Bai, F. Yang, and Z. Zhou, "Ultra-compact hybrid plasmonic mode convertor based on unidirectional eigenmode expansion," Opt. Lett. **45**, 803–806 (2020).

17. D. Dai, Y. Tang, and J. E. Bowers, "Mode conversion in tapered submicron silicon ridge optical waveguides," Opt. Express **20**, 13425–13439 (2012).

18. D. Dai and M. Zhang, "Mode hybridization and conversion in silicon-on-insulator nanowires with angled sidewalls," Opt. Express **23**, 32452–32464 (2015).

19. Z. Mohammed, B. Paredes, and M. Rasras, "Effect of process parameters on mode conversion in submicron tapered silicon ridge waveguides," Appl. Sci. **11**, 2366 (2021).

20. H.-J. Hagemann, W. Gudat, and C. Kunz, "Optical constants from the far infrared to the x-ray region: Mg, Al, Cu, Ag, Au, Bi, C, and Al_2O_3," J. Opt. Soc. Am. **65**, 742–744 (1975).

21. M. M. Dumitrescu and M. D. Guina, "Effective index method for the computation of the propagation constant and electromagnetic field distribution in z-uniform dielectric or semiconductor waveguides," Proc. SPIE **3405**, 922–925 (1998).

22. K. S. Chiang, "Analysis of the effective-index method for the vector modes of rectangular-core dielectric waveguides," IEEE Trans. Microw. Theory Tech. **44**, 692–700 (1996).

23. H. Guan, Y. Ma, R. Shi, A. Novack, J. Tao, Q. Fang, A. E.-J. Lim, G.-Q. Lo, T. Baehr-Jones, and M. Hochberg, "Ultracompact silicon-on-insulator polarization rotator for polarization-diversified circuits," Opt. Lett. **39**, 4703–4706 (2014).

24. K. Goi, A. Oka, H. Kusaka, K. Ogawa, T.-Y. Liow, X. Tu, G.-Q. Lo, and D.-L. Kwong, "Low-loss partial rib polarization rotator consisting only of silicon core and silica cladding," Opt. Lett. **40**, 1410–1413 (2015).

25. A. Nanotools, *Dedicated Runs and Capabilities in Development* (2023).

26. L. C. Kimerling, "The international integrated photonic systems roadmap: defining the destination and the path (conference presentation)," Proc. SPIE **11284**, 112840C (2020).

27. M. Polyanskiy, Refractiveindex.Info Database (2023), https://refractiveindex.info.

28. P. R. West, S. Ishii, G. V. Naik, N. K. Emani, V. M. Shalaev, and A. Boltasseva, "Searching for better plasmonic materials," Laser Photon. Rev. **4**, 795–808 (2010).

29. S. Chakravarty, J. Midkiff, K. Yoo, C.-J. Chung, A. Rostamian, and R. T. Chen, "Compact integrated photonic components for lambda= 3-15 micron," Proc. SPIE **10921**, 109210D (2019).

30. Z. Cheng, J. Wang, Z. Yang, H. Yin, W. Wang, Y. Huang, and X. Ren, "Broadband and high extinction ratio mode converter using the tapered hybrid plasmonic waveguide," IEEE Photon. J. **11**, 4900608 (2019).